Dystroglycan Matrix Receptor Function in Cardiac Myocytes Is Important for Limiting Activity-Induced Myocardial Damage

Daniel E. Michele, Zhyldyz Kabaeva, Sarah L. Davis, Robert M. Weiss, Kevin P. Campbell

Rationale: Genetic mutations in a number of putative glycosyltransferases lead to the loss of glycosylation of dystroglycan and loss of its laminin-binding activity in genetic forms of human muscular dystrophy. Human patients and glycosylation defective *myd* mice develop cardiomyopathy with loss of dystroglycan matrix receptor function in both striated and smooth muscle.

Objective: To determine the functional role of dystroglycan in cardiac muscle and smooth muscle in the development of cardiomyopathy in muscular dystrophies.

Methods and Results: Using cre/lox–mediated gene targeting, we show here that loss of dystroglycan function in ventricular cardiac myocytes is sufficient to induce a progressive cardiomyopathy in mice characterized by focal cardiac fibrosis, increase in cardiac mass, and dilatation ultimately leading to heart failure. In contrast, disruption of dystroglycan in smooth muscle is not sufficient to induce cardiomyopathy. The specific loss of dystroglycan function in cardiac myocytes causes the accumulation of large, clustered patches of myocytes with membrane damage, which increase in number in response to exercise-induced cardiac stress, whereas exercised mice with normal dystroglycan expression accumulate membrane damage limited to individual myocytes.

Conclusions: Our findings suggest dystroglycan function as an extracellular matrix receptor in cardiac myocytes plays a primary role in limiting myocardial damage from spreading to neighboring cardiac myocytes, and loss of dystroglycan matrix receptor function in cardiac muscle cells is likely important in the development of cardiomyopathy in glycosylation-deficient muscular dystrophies. (*Circ Res*. 2009;105:984-993.)

Key Words: heart failure ■ cardiomyopathy ■ adhesion molecules ■ muscular dystrophy

Clinically defined cardiovascular disease occurs in more than 70% to 90% of muscular dystrophy patients with defects in the dystrophin–glycoprotein complex (DGC), and heart failure is the second leading cause of death in these patients.[1] The DGC contains a key transmembrane glycoprotein, dystroglycan (DG), which is believed to link the intracellular protein dystrophin to the extracellular matrix. DG is composed of α and β subunits. β-DG binds intracellularly to dystrophin, which binds the actin cytoskeleton, and binds extracellularly to α-DG. The heavily glycosylated α-DG binds tightly to extracellular matrix proteins, such as laminin, with high affinity. In muscle cells, the DGC also contains a sarcoglycan–sarcospan complex composed of sarcoglycan proteins (α, β, γ, and δ in striated muscle) and sarcospan. Whereas mutations in dystrophin and each of the four sarcoglycans can cause Duchenne/Becker and limb girdle muscular dystrophies respectively, no mutations in DG have been identified as a cause of human disease.

The distribution of DG and the DGC in both cardiac and vascular smooth muscle have raised questions about whether the cardiomyopathy present in muscular dystrophy is primary to cardiac muscle dysfunction or might be a consequence of changes in vascular function. Sarcoglycan-deficient mice and hamsters show coronary vasospasm,[2–4] and coronary dysfunction has been suggested to be the primary cause of cardiomyopathy.[2,3] However, it is possible coronary vasospasm or peripheral vasoconstriction could be secondary to the release of factors by diseased cardiac myocytes or skeletal muscle cells.[5,6] In support of this hypothesis, transgenic overexpression of δ-sarcoglycan in cardiac myocytes of the δ-sarcoglycan knockout mouse appears to slow or prevent histological evidence of cardiomyopathy.[7] The fact that mutations in δ-sarcoglycan can cause dilated cardiomyopathy without skeletal muscle disease,[8] and the presence of an alternative sarcoglycan complex in smooth muscle[9] suggests sarcoglycans may have a unique function in the cardiovascular

Original received April 20, 2009; revision received September 8, 2009; accepted September 10, 2009.

From the Departments of Molecular and Integrative Physiology (D.E.M., Z.K.) and Internal Medicine (D.E.M.), University of Michigan, Ann Arbor; and Departments of Molecular Physiology and Biophysics (S.L.D., K.P.C.), Neurology (K.P.C.), and Internal Medicine (R.M.W., K.P.C.) and Howard Hughes Medical Institute (S.L.D., K.P.C.), University of Iowa, Iowa City.

Correspondence to Daniel Michele, PhD, Assistant Professor, Department of Molecular and Integrative Physiology, Department of Internal Medicine, University of Michigan, 7732C Medical Science II, 1301 E Catherine St, Ann Arbor, MI 48109-0622. E-mail dmichele@umich.edu

Circulation Research **is available at http://circres.ahajournals.org** **DOI: 10.1161/CIRCRESAHA.109.199489**

system, acting through a mechanism that is distinct from the function of DG and dystrophin glycoprotein complex function.

Although DG mutations have not been linked to human disease, mutation in genes including POMGnT-1, POMT1, POMT1, FKTN, LARGE, and FKRP can cause a broad spectrum of disease severity, ranging from severe congenital muscular dystrophy, such as Walker–Warburg syndrome, to mild LGMD, such as LGMD2I. The proteins encoded by these genes all have homology to glycosyltransferases and mutations in these genes lead to a convergent loss of glycosylation of α-DG and a loss of DG function as a receptor for its known extracellular matrix ligands.[10] Myodystrophy (*myd*) mice, resulting from mutations in LARGE, demonstrate hypoglycosylation of α-DG and abnormal DG ligand binding in skeletal muscle, which is biochemically similar to that of human muscular dystrophy patients with glycosylation-deficient muscular dystrophy.[10,11] LARGE is believed to be a "master" regulator of the glycosylation pathway necessary for DG glycosylation and function.[12] Studies have shown that *myd* mice develop histological evidence of cardiomyopathy and a loss of glycosylated DG in the heart, similar to the cardiomyopathy and glycosylation deficiency observed in human patients.[13,14] The molecular mechanisms that lead to cardiomyopathy in these disorders are unknown.

In the present study, we show that glycosylation-deficient *myd* mice have impaired DG glycosylation in smooth muscle, including coronary blood vessels, and a quantitatively comparable loss of high-affinity laminin-binding activity in both cardiac and smooth muscle. To address the significance of loss of DG function with respect to the cardiomyopathy in glycosylation-deficient muscular dystrophies, we used cre/lox technology to disrupt the DG gene in the cardiovascular system in a tissue specific manner. Our results indicate that gene-targeted loss of DG function specifically in cardiac myocytes is sufficient to cause cardiomyopathy in mice. Moreover, in actively contracting myocardium and after increased cardiac stress induced by exercise, DG appears to play an important role in limiting cardiac myocyte membrane damage to individual cells, and loss of its function as an extracellular matrix receptor in mice results in expansion of myocardial damage to nearest neighboring cells.

Methods

An expanded Methods section is available in the Online Data Supplement at http://circres.ahajournals.org.

Mice

B6C3Fe-a/a-LARGE*myd* mice were obtained from The Jackson Laboratories. Mice expressing Cre recombinase under control of the myosin light chain 2v regulatory region (MLC2vcre)[15] or using the smooth muscle myosin heavy chain (MHC) promoter[16] were kind gifts from Dr Kenneth Chien and Dr Gary Owens, respectively. Mice deficient for DAG1 were generated by mating male mice heterozygous for the cre transgene and homozygous for the DAG1 floxed allele, with females that were homozygous for the DAG1 floxed allele.[17] The mice from these crosses were born in the predicted Mendelian ratios (see Supplemental Methods). All comparisons were made on age- and sex-matched littermate mice. All procedures were approved by the University Committee for the Use and Care of Animals.

DG Glycosylation, DGC Protein Expression, and Laminin-Binding Activity

DG glycosylation, protein expression, immunolocalization, and laminin-binding activity were analyzed in wheat germ agglutinin–enriched glycoprotein preparations as previously described.[10]

Non-standard Abbreviations and Acronyms

BW	body weight
DGC	dystrophin–glycoprotein complex
DG	dystroglycan
EBD	Evan's blue dye
HW	heart weight
LGMD	limb girdle muscular dystrophy
MHC	myosin heavy chain
MLC2v	myosin light chain 2v
myd	myodystrophy
SMMHC	smooth muscle myosin heavy chain
WT	wild type

In Vivo Echocardiography

Mice were analyzed by in vivo echocardiography while conscious as previously described.[18]

In Vivo Assessment of Myocardial Membrane Damage

Five hours before a 1-hour graded treadmill exercise session, mice (<5 months of age) were given an IP injection of 0.1 mg/g Evan's blue dye (EBD) in saline. Eighteen hours after injection, with or without exercise, hearts were removed, and 4 cryosections >250 to 300 μm apart were obtained. Immunostaining with anti–laminin 1 antibody (Sigma, 1:1000) was used to show cell boundaries and identify cells with dye uptake.

Results

Glycosylation-Deficient Muscular Dystrophy Mice Show Loss of DG Glycosylation in Both Cardiac and Smooth Muscle

Hearts from *myd* mice at 10 months of age displayed evidence of significant but focal interstitial myocardial collagen deposition, consistent with cardiac remodeling that occurs following myocardial damage (Figure 1A). To address how the loss of LARGE activity affects DG glycosylation in *myd* mice across tissues, the apparent molecular weight shifts of α-DG protein from tissues of wild-type (WT) and *myd* mice were compared using an antibody against the core α-DG protein. In addition to skeletal muscle and brain as previously reported,[10] both cardiac muscle and smooth muscle α-DG from *myd* mice (using bladder as a source of tissue composed primarily of smooth muscle), were also markedly reduced in molecular weight compared to their littermate WT controls (Figure 1B and 1D). In contrast, other tissues such as kidney, lung, testes, spleen, and liver did not show as large a shift in molecular weight of α-DG, although more subtle shifts were still observed in the absence of LARGE activity (Online Figure I). By comparing the amounts of IIH6-reactive α-DG to the amount of α-DG recognized by the core α-DG antibody, levels of the highly glycosylated form of α-DG (recognized by IIH6) were high in WT skeletal muscle, brain, heart, smooth muscle, and kidney but barely detectable in lung, testes, spleen and liver (Figure 1B and 1C; Online Figure I). The reactivity of IIH6 antibody was tightly correlated with laminin-binding activity of α-DG detected by laminin overlay assay (Figure 1C and Online

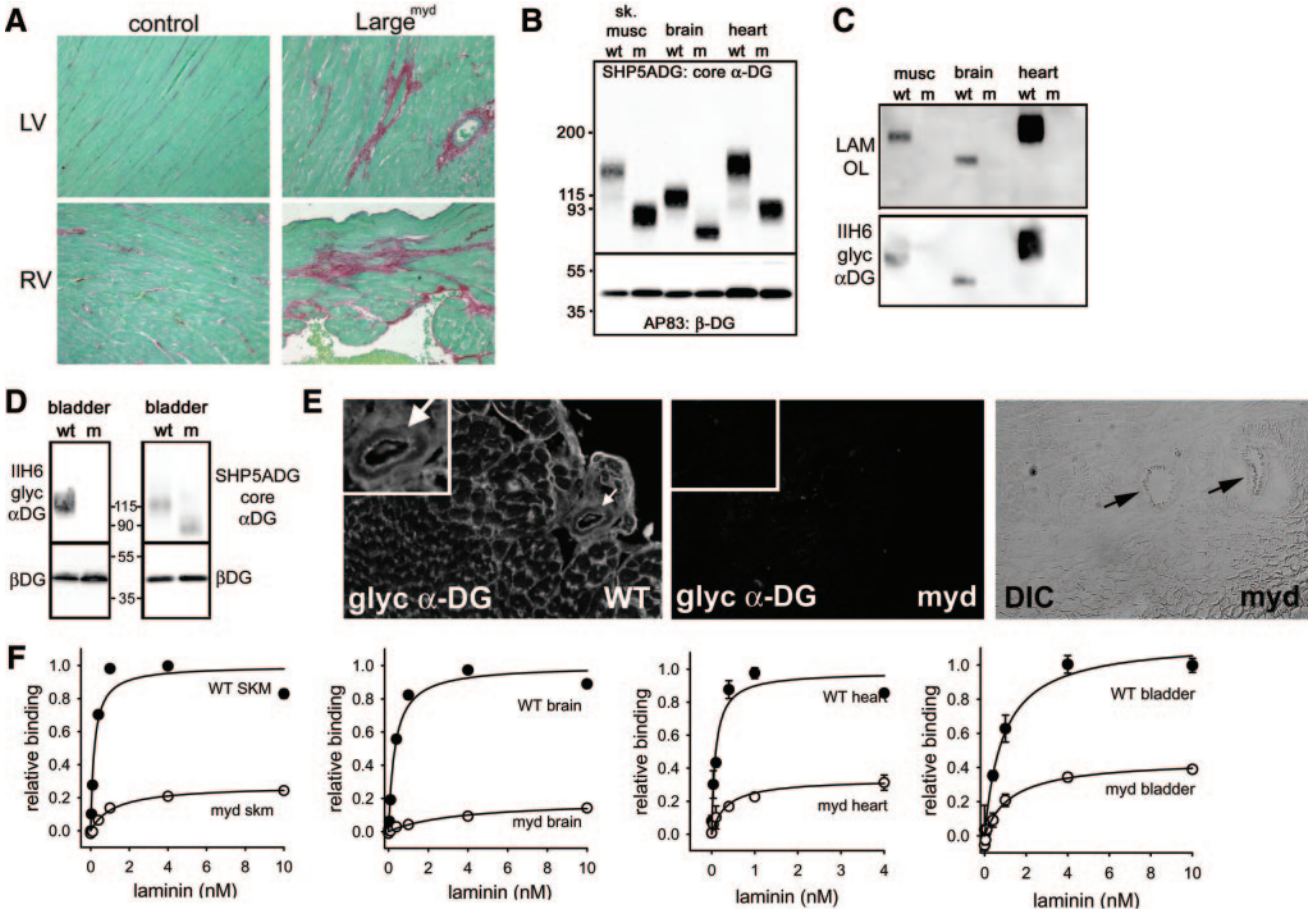

Figure 1. Distribution of DG glycosylation deficiency and laminin-binding activity in the cardiovascular system and other tissues of glycosylation-deficient *myd* mice. A, Myocardium of 10-month-old *myd* mice shows focal areas of collagen deposition. Collagen was stained with Sirius red and counterstained with fast green. LV indicates left ventricle; RV, right ventricle. B, Assessment of α-DG protein expression and molecular weight in tissues of *myd* mice using an antibody that recognizes the core α-DG protein. C, The fully glycosylated α-DG (recognized by IIH6) and laminin-binding glycoform (determined by laminin overlay assay) of α-DG are easily detected in muscle, heart, and brain. D, Glycosylation of α-DG is also markedly affected in smooth muscle (from bladder) of *myd* mice, as indicated by a loss of IIH6 staining and a reduction in molecular weight. E, IIH6 immunostaining in the myocardium of *myd* mice reveals a loss of staining at the plasma membrane in cardiac myocytes and a loss of staining in coronary blood vessels (arrows). A differential interference contrast (DIC) image of the *myd* tissue demonstrates 2 coronary vessels are in the field of view. F, High-affinity laminin-binding activity is markedly reduced in heart and smooth muscle of *myd* mice ($P<0.05$ at 1 to 10 nmol/L laminin points). Data were normalized to the peak-binding activity in littermate WT animals to allow comparisons of total activity and relative affinity. All data shown are means±SD (n=3), and in cases in which the error bars are smaller than the data points, the SD was less than 0.04. The biochemical data in B through F were performed in mice age 14 to 20 weeks.

Figure I). In each adult tissue, where the IIH6-reactive, laminin-binding form of α-DG was highly expressed in WT mice, the IIH6 reactive α-DG and laminin-binding activity by overlay assay was undetectable in samples from *myd* mice. Loss of α-DG glycosylation did not appear to markedly impact the expression levels of the DG peptide in these tissues. Staining of tissues from *myd* mice, including the myocardium, demonstrate that the glycosylated form of α-DG is lost from all tested vascular smooth muscle including coronary blood vessels (Figure 1E). This loss of DG glycosylation results in a significant loss of total high-affinity laminin-binding activity in skeletal, cardiac and smooth muscle, and brain (Figure 1F). Together, these results demonstrate that LARGE activity is necessary for the type of DG glycosylation that is required for its function as an extracellular matrix receptor in: striated muscle (including the heart); smooth muscle; the nervous system; and, to a lesser extent, the kidney.

Genetic Disruption of the DG Gene in the Cardiac Myocytes or Smooth Muscle Leads to a Tissue-Specific Loss of DG Expression

To determine the significance that the loss of DG function in cardiac or vascular smooth muscle has for the development of cardiomyopathy, mice bearing an allele of the DG gene (DAG1) flanked by loxP sites (L/L) were crossed with mice that express cre-recombinase in either cardiac ventricular muscle (MLC2vcre-L/L) or in all smooth muscle (SMMHC-cre-L/L). In MLC2vcre-L/L mice, there was loss of DG expression in nearly all ventricular cardiac myocytes, whereas coronary vascular smooth muscle expression of DG was maintained (Figure 2A). A small percentage of cardiac myocytes (21 of 2350 myocytes in random fields from 3 animals) showed residual DG expression (Figure 2A). Conversely, in the SMMHCcre-L/L mice showed complete loss of DG staining in vascular smooth muscle in coronary

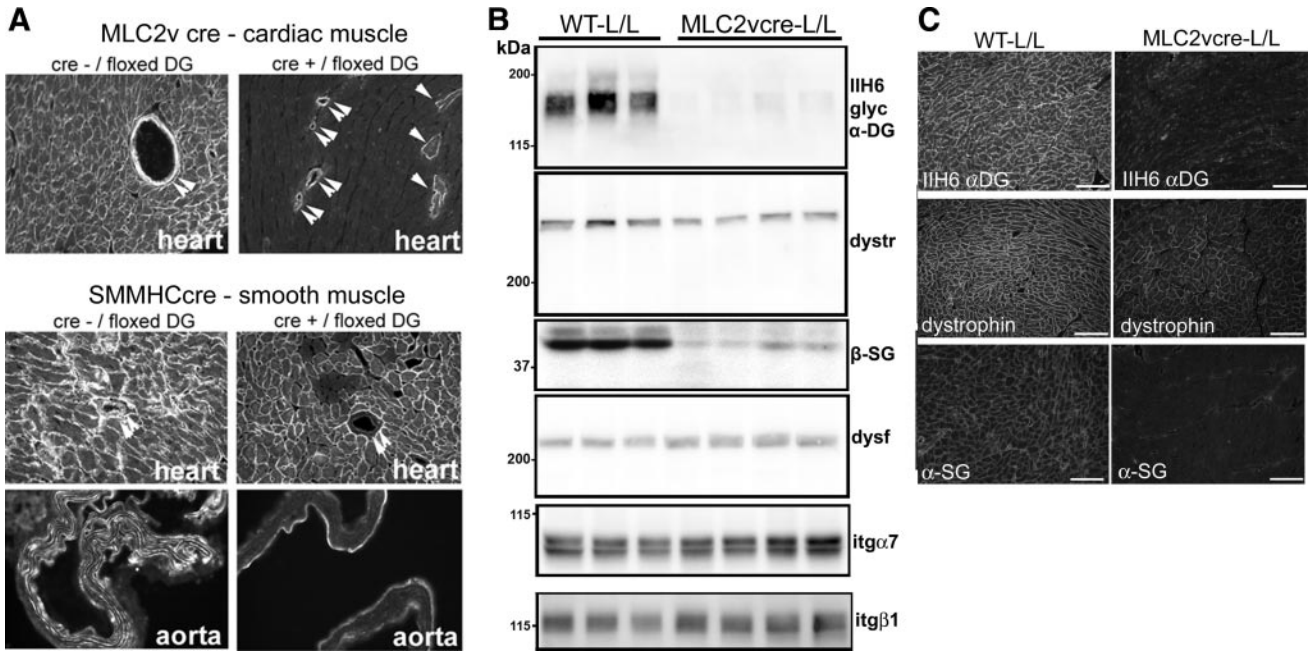

Figure 2. Targeted tissue-specific deletion of DG gene expression in cardiac and smooth muscle. A, Immunostaining with an antibody against β-DG. Double arrows indicate smooth muscle in coronary vessels. Single arrows indicate cardiac myocytes expressing residual β-DG. In MLC2vcre-L/L mice, the field shown was specifically chosen to show the residual positive cells, whereas most fields were negative for DG expression. In SMMHCcre-L/L mice, DG expression was not detected in smooth muscle. A very small portion of cardiac myocytes also showed gene targeting, most likely attributable to the transient expression of smooth muscle markers in cardiac myocytes during development, although most fields analyzed showed normal DG expression in all cardiac myocytes. B, Analysis of DG, dystrophin (dystr), dysferlin (dysf), β-sarcoglycan (β-SG), and integrin (itg) protein expression in MLC2vcre-L/L ventricular myocardium compared to littermate L/L (WT) mice. Each lane represents ventricular muscle from a different animal. C, Immunofluorescence localization of dystrophin is retained at the plasma membrane of cardiac myocytes in MLC2vcre-L/L mice despite loss of DG expression, whereas α-sarcoglycan expression is reduced. Samples in A through C were from mice aged 14 to 20 weeks.

vessels, the aorta (although largely collagen-based tunica externa remained positive), and bladder smooth muscle (Figure 2A; Online Figure II). Whereas nearly all ventricular myocytes in the SMMHCcre-L/L mice exhibited normal DG expression, a small subset of ventricular myocytes in this mouse was targeted by this promoter (Figure 2A). These targeted myocytes were observed in sample sections of 2 of 4 SMMHCcre-L/L hearts examined, but only 18 and 27 myocytes were disrupted in an entire cross section of the heart in those samples. This is likely attributable to the short-lived, developmental expression of the smooth muscle MHC gene in a subset of myocytes that has been characterized previously.[16]

To determine how loss of DG protein expression impacted the expression of the DGC in cardiac muscle, DGC protein expression in ventricles of MLC2vcre-L/L mice was examined (Figure 2B). DG expression was reduced 93.8±1.5% (means±SEM, n=4, $P<0.05$). Somewhat surprisingly, the loss of DG protein expression in cardiac myocytes by gene targeting failed to cause a corresponding marked reduction in dystrophin expression, and the expressed dystrophin was retained at the sarcolemma (Figure 2C), even though DG is a direct binding partner of dystrophin in the DGC. In contrast, sarcoglycan expression levels were reduced to a much greater extent than the dystrophin expression levels, although not lost completely in MLC2vcre-L/L mice. These results suggest that dystrophin may interact with other proteins in cardiac muscle cells to confer dystrophin protein stability. There was also a slight increase in dysferlin expression (37% increase, $P<0.05$), but no change in α7 or β1 integrin expression ($P>0.05$), as measured by densitometry, in MLC2vcre-L/L animals. In SMMHCcre-L/L mice, immunofluorescence staining also revealed a reduction of β-sarcoglycan immunofluorescence staining in vascular smooth muscle and bladder smooth muscle accompanying loss of DG expression in SMMHCcre-L/L mice (Online Figure II).

Tissue-Specific Loss of DG Expression in Cardiac Myocytes Is Sufficient to Cause a Cardiomyopathic Phenotype in Mice

Ten-month-old MLC2vcre L/L mice showed marked cardiac pathology, including myocardial cell degeneration marked by eosinophilic myocytes, infiltration of mononuclear cells in a subset of cases with severe pathology, and significant focal collagen deposition (Figure 3A). All hearts from MLC2vcre-L/L mice examined appeared enlarged in cross section and a subset showed focal thinning of the left ventricular wall. Consistent with these histological observations, MLC2vcre-L/L mice showed a 65% increase in heart weight (HW)/body weight (BW) ratios compared to L/L mice (Figure 3B) and a significant increase in cardiac fibrosis, with nearly 9% of the myocardium being replaced with focal fibrotic tissue in 10-month-old mice (Figure 3C). Despite the focal nature of the fibrosis, microfil perfusion experiments did not reveal evidence of coronary vasospasms (Online Figure III). SMMHCcre-L/L mice at 10 months of age failed to show alterations in cardiac mass or any pathology by histological staining (Figure 3).

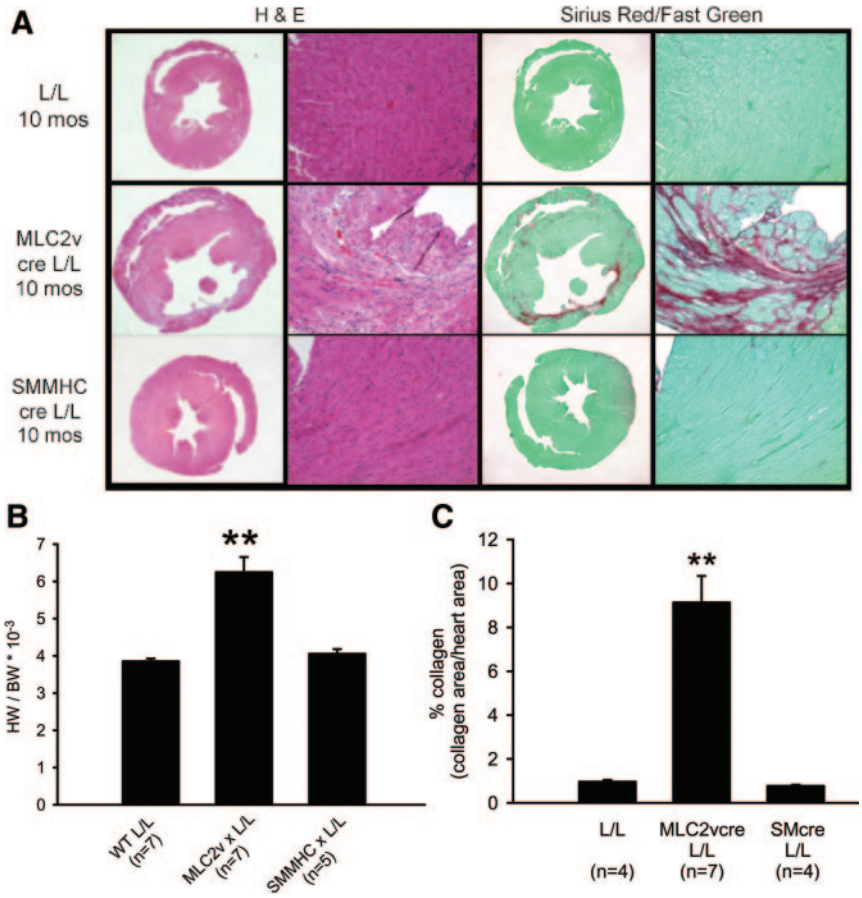

Figure 3. Mice with cardiac myocyte restricted deletion of DG gene show morphological evidence of a cardiomyopathic phenotype. A, Morphological analysis of hearts from littermate control mice (L/L), MLC2vcre-L/L mice, and SMMHCcre-L/L mice at 10 months of age. Formalin-fixed heart sections were stained with hematoxylin/eosin (left) to assess gross histology and with Sirius red (right) for collagen deposition. MLC2vcre-L/L mice show evidence of increased myocardial damage, ventricular wall thinning, enlarged hearts, and collagen deposition, whereas SMMHCcre-L/L mice were indistinguishable from L/L mice. B, HW/BW ratios at 10 months age revealed a significant increase in cardiac mass in MLC2vcre-L/L animals. BW was unchanged in the 3 groups (46.4±1.8 g, WT; 47.4±2.5 g, MLC2vcre-L/L; 47.2±1.1 g, SMMHCcre-L/L; $P>0.05$). C, Collagen deposition was quantified using image analysis of Sirius red–stained sections and revealed a significant increase in fibrotic area in MLC2vcre-L/L animals. $^{**}P<0.001$ by ANOVA and a Bonferroni's post hoc test compared to both L/L and SMMHCcre-L/L mice. Data shown are means±SEM.

Consistent with the morphological findings, murine echocardiography showed the cardiac mass and end diastolic volume were significantly increased in MLC2vcre-L/L mice (Figure 4). The ratio of the end diastolic volume to mass was also increased, confirming these mice experienced pathological chamber dilation as opposed to a mere increase in overall heart size. MLC2vcre-L/L mice also showed a significant impairment of systolic function, as evidenced by a reduction in the left ventricular ejection fraction. In contrast, the loss of DG function in smooth muscle had no measureable impact on

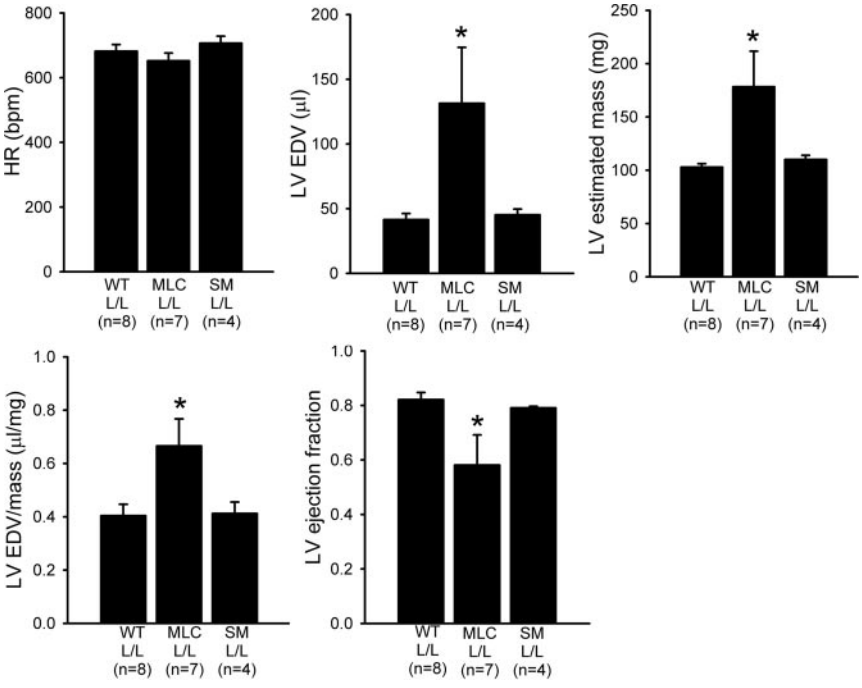

Figure 4. Mice with cardiac-restricted deletion of the DG gene show evidence for a cardiomyopathic phenotype by echocardiography. Echocardiography was performed on 10-month-old L/L littermate mice, MLC2vcre-L/L, and SMMHCcre-L/L mice. MLC2vcre-L/L mice displayed a significant increase in end diastolic volume (EDV) that exceeded the measured increase in cardiac mass and a decrease in ejection fraction that suggested an overall functional dilated cardiomyopathic phenotype. Data shown are means±SEM. $^{*}P<0.05$ by ANOVA and a Bonferroni's post hoc test compared to both L/L and SMMHCcre-L/L mice. HR indicates heart rate; LV, left ventricular.

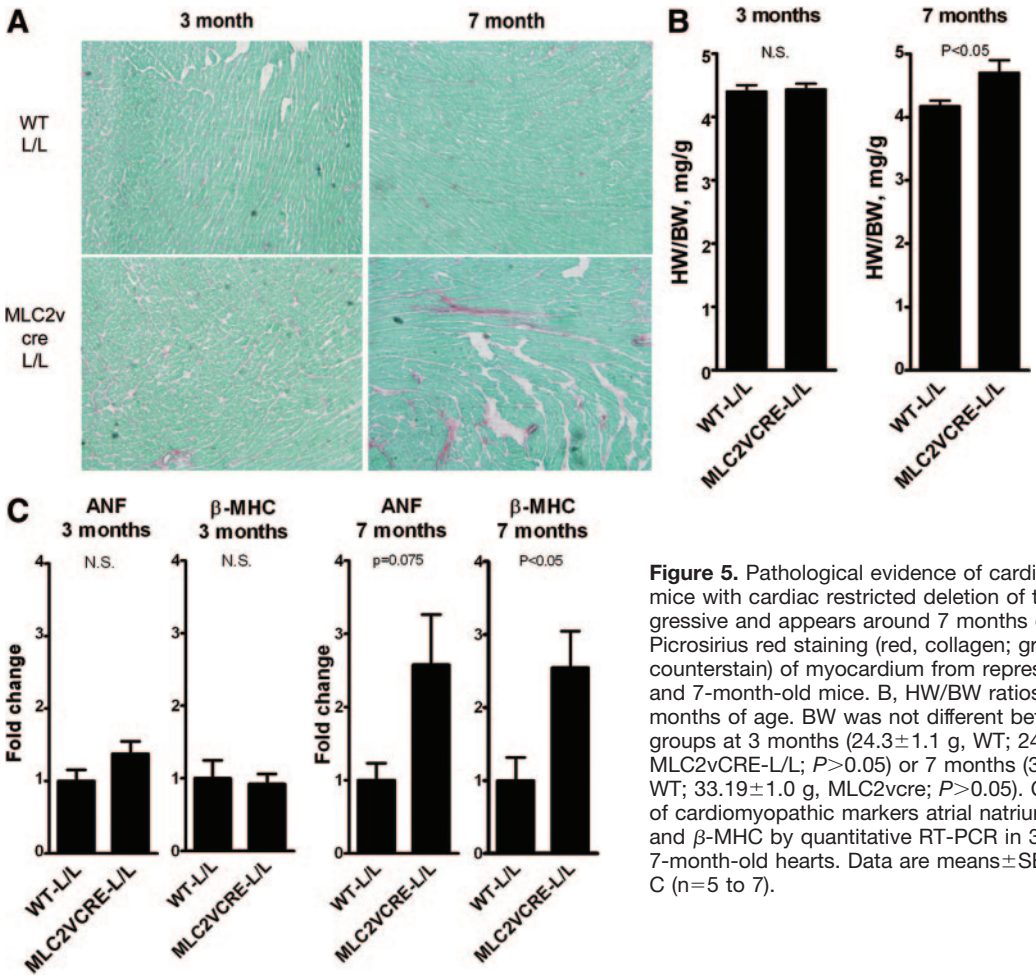

Figure 5. Pathological evidence of cardiomyopathy in mice with cardiac restricted deletion of the DG is progressive and appears around 7 months of age. A, Picrosirius red staining (red, collagen; green, tissue counterstain) of myocardium from representative 3- and 7-month-old mice. B, HW/BW ratios at 3 and 7 months of age. BW was not different between the 2 groups at 3 months (24.3±1.1 g, WT; 24.52±0.9 g, MLC2vCRE-L/L; $P>0.05$) or 7 months (34.7±1.1 g, WT; 33.19±1.0 g, MLC2vcre; $P>0.05$). C, Expression of cardiomyopathic markers atrial natriuretic factor and β-MHC by quantitative RT-PCR in 3- and 7-month-old hearts. Data are means±SEM for B and C (n=5 to 7).

cardiac function as measured by echocardiography. Together, these echocardiography findings support the conclusion that the loss of DG function in cardiac myocytes is necessary and sufficient to cause a functional dilated cardiomyopathy.

Examining mice at several ages indicated that the first detectable signs of cardiomyopathy by histology and pathological markers in MLC2vcre-L/L mice occurs around seven moths of age. MLC2vcre-L/L mice at 3 months of age appear histologically and morphologically normal (Figure 5). MLC2vcre-L/L mice at 7 months begin to show small focal areas of fibrosis and a small increase in HW/BW ratio. Furthermore, MLC2vcre-L/L mice at 7 months of age show significant activation of β-MHC gene expression, which as important molecular marker of cardiomyopathic remodeling

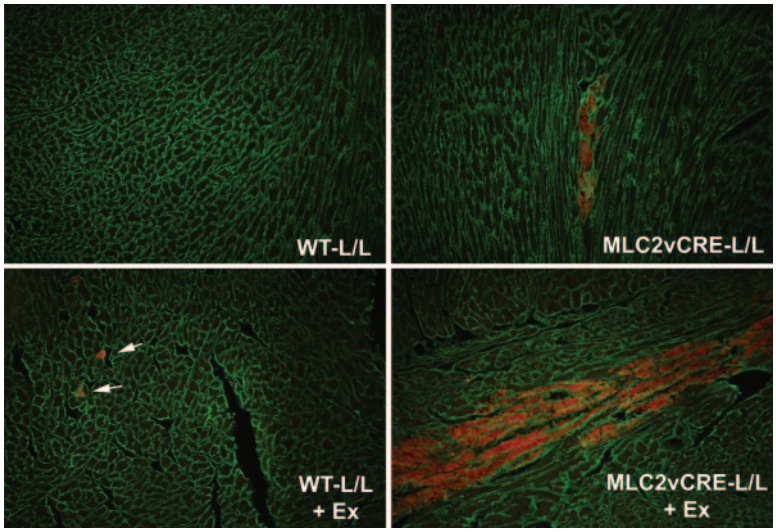

Figure 6. Acute myocyte damage in WT and MLC2vcre-L/L in response to exercise stress. Representative images showing EBD uptake (red) in sedentary and exercised (+Ex) WT and MLC2vcre-L/L mice. A pan-laminin antibody was used to outline the cell boundaries to score EBD within individual myocytes, and fibrosis was not observed in hearts in which these sections were taken. Patches of myocytes in MLC2vcre-L/L mice consisted of a number of contacting neighboring cells with similar orientation of their longitudinal axis. Note that there was no significant difference in the staining with laminin, suggesting an intact basal lamina.

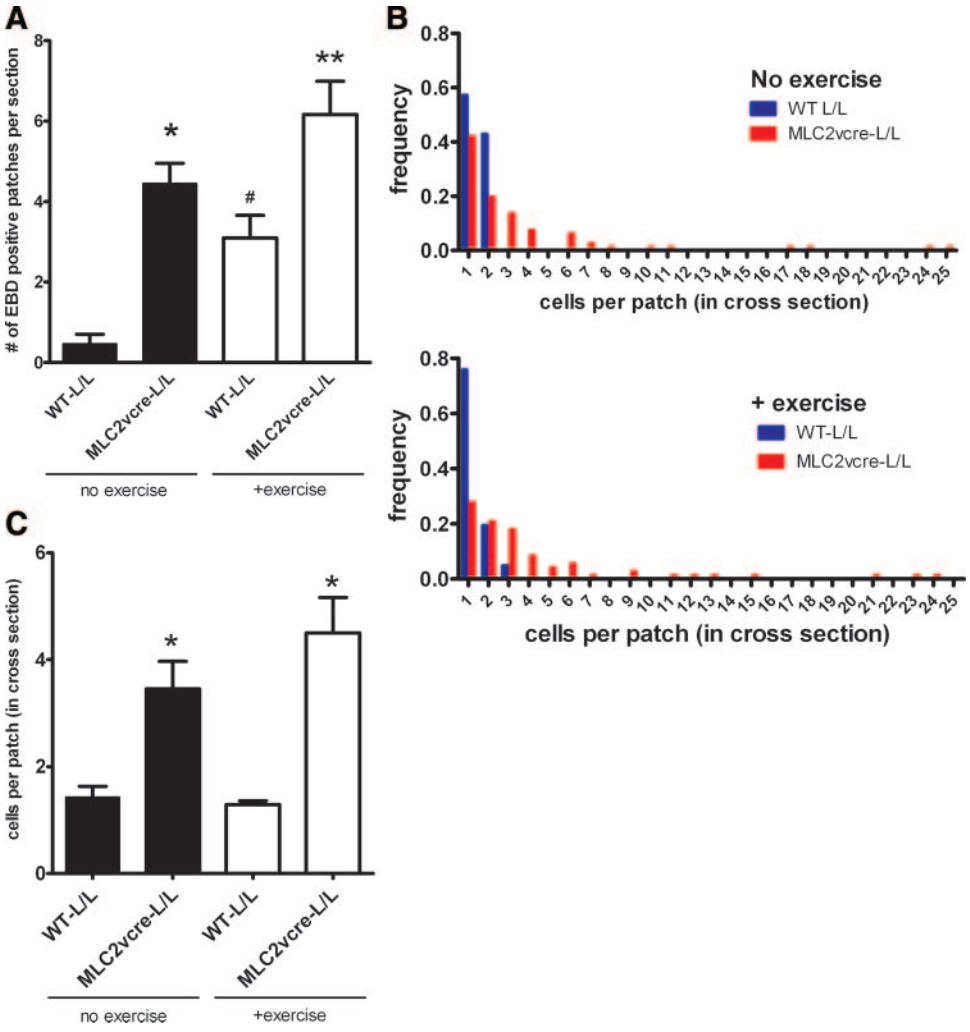

Figure 7. Loss of DG function in cardiac myocytes causes expansion of myocardial damage to neighboring myocytes. The scoring of EBD patches is described in detail in Methods. A, The number of EBD-positive patches per section was significantly increased in MLC2vcre-L/L mice compared to WT animals and was significantly increased by exercise in both groups. Data are means±SEM. *$P<0.01$ vs WT-L/L no exercise; #$P<0.01$ vs WT L/L; **$P<0.05$ vs all 3 other groups. B, Frequency distribution of the size of EBD-positive patches in cross-section of WT and MLC2vcre-L/L mice, with and without exercise. C, Summary of the numbers of EBD-positive cells per patch in all patches scored. Data are means±SEM (n=64 to 87), except WT-L/L no exercise, where only 8 total patches were found. *$P<0.01$ vs WT-L/L exercised.

associated with both cardiac hypertrophy and fibrosis,[19] but mice at 3 months of age showed no activation of β-MHC or ANF (Figure 5). These data suggest that cardiomyopathy develops progressively in adult animals because of cumulative effects of lifetime loss of DG in cardiac myocytes, rather than a congenital defect in young animals.

DG Expression in Cardiac Myocytes Is Necessary for Limiting Stress-Induced Cardiac Myocyte Damage From Spreading to Nearest Neighbor Cells

Because loss of DG expression in cardiac myocytes and loss of DG laminin-binding activity in *myd* mice is sufficient to cause a progressive cardiomyopathy characterized by focal fibrosis, we hypothesized that the function of DG as an extracellular matrix receptor in cardiac myocytes might play a primary role in preventing myocardial damage in young animals that accumulates with age, leading to cardiomyopathic remodeling. To test this hypothesis, young WT and MLC2vcre-L/L mice (<5 months old, before detectable fibrosis or cardiac histopathology) were examined for sarcolemma damage in cardiac myocytes, by EBD uptake in sedentary and acutely exercised animals. In WT, unexercised animals, very few EBD-positive cells were observed, with most sections devoid of any dye uptake. Interestingly, in WT animals, EBD-positive myocytes were consistently observed after exercise, but the sarcolemma damage was almost always limited to single isolated myocytes. In contrast, MLC2vcre-L/L animals had a markedly different pattern of EBD uptake both in exercised and unexercised mice, where EBD uptake seemed to occur in large groups of neighboring cells, or cell "patches"(Figure 6). We also noted the patches of membrane damage in MLC2vcre-L/L mice appeared to be limited to cardiac myocytes that were organized in similar orientations of their longitudinal, or mechanical axis (Figure 6). To examine this curious pattern of dye uptake in more detail, the total number of patches of damaged cells as small as one cell, and the size of those patches were quantified (Figure 7). These results showed that acute exercise was able to produce a significant number of EBD-positive cells in WT animals, but these patches were typically observed as one isolated cardiac myocyte (Figure 7). In contrast, loss of DG function resulted in slightly greater numbers of patches both in sedentary and exercised animals but, more significantly, a dramatic increase in the size of those patches up to patch sizes that exceeded 25 contacting cells in cross sections of myocardium from MLC2vcre-L/L mice (Figure 7). Note that the measurements of patch size were sampled in cross-sections,

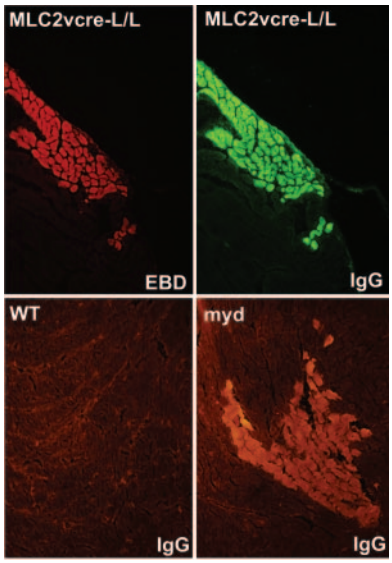

Figure 8. *Myd* mice show focal patches of cardiac myocyte membrane damage. The upper images show cardiac myocytes demonstrating EBD uptake; the images also show uptake of large extracellular proteins such as immunoglobulin. In the lower images, sedentary *myd* mice show patches of membrane damage, marked by immunoglobulin staining, similar to that observed in MLC2vcre-L/L animals.

suggesting that these patches likely contain a significantly larger number of cells in 3 dimensions. Also, the greater number of patches observed in MLC2vcre-L/L animals could, in part, be attributable to the increased size of the patches increasing likelihood of observing a patch in a random section. The mean patch size in each genotype was not statistically different in control and exercised animals, indicating the size of the patch was not influenced by exercise stress. Taken together, these results suggest that cardiac membrane damage and uptake of EBD can occur even in WT mice in response to increased activity, but the primary role of DG in cardiac myocytes is to protect against the expansion of that initial myocyte damage to neighboring cardiac myocytes. Myocytes that take up EBD also take up large proteins from the extracellular space including immunoglobulin (Figure 8). By marking membrane damage with immunoglobulin, Figure 8 shows that sedentary *myd* mice also have large patches of neighboring myocytes with membrane damage similar to that observed in sedentary MLC2vcre-L/L animals. Therefore, loss of the function of DG as an extracellular matrix receptor in cardiac myocytes appears critical to preventing expansion of initial myocyte membrane damage to neighboring cardiac myocytes.

Discussion

The mechanistic role of DG function in muscular dystrophy and cardiomyopathy, and the exact function of DG in striated muscle and smooth muscle, is still debated. Although cytoskeletal to matrix linkages through DG and other receptors have been proposed to be critical for muscle cell survival,[20] the association of the dystrophin glycoprotein complex with signaling molecules such as kinase cascades and nitric oxide synthase suggest several possible significant roles in striated and vascular smooth muscle.[21,22] Our results indicate that the loss of DG function in cardiac myocytes results in increased myocyte membrane damage in response to increased activity and is sufficient to cause a progressive dilated cardiomyopathy and that loss of DG function in smooth muscle does not cause a detectable cardiac phenotype.

Despite the uniform genetic deletion of DG function in myocytes (Figures 2 and 7), the membrane damage observed in MLC2vcre-L/L mice is not uniform and occurs in distinct focal patches of adjacent myocytes, rather than just randomly membrane-damaged myocytes throughout the myocardium. Patchy areas of cell membrane damage were also observed in *myd* mice in the presence of uniform loss of DG laminin-binding function (Figures 1 and 8). Previous studies in sarcoglycan deficient animals suggested the cardiomyopathy was correlated with coronary vasospasm and loss of sarcoglycan expression in smooth muscle.[2,3] However, we did not observe evidence of coronary vasospasm by microfil perfusion in MLC2vcre-L/L mice, and DG and DGC expression in smooth muscle was normal in MLC2vcre-L/L mice. Furthermore, no patches of myocardial damage or fibrosis were observed in SMMHCcre-L/L mice. We also demonstrate that exercise can induce surprisingly significant numbers of EBD-positive cells in WT mice compared to unexercised WT mice, but the damage is always limited to 1 or 2 cells. Taken together, these data suggest that the interaction of DG with the extracellular matrix is required for stabilizing neighboring cells against sarcolemma injury and preventing expansion of membrane damage to neighboring cells in response to an individual cell becoming damaged. Because significant focal patches of membrane damage are observed in younger ML2vcre-L/L mice, even in the absence of exercise, the accumulation of focal myocardial damage even under sedentary conditions is likely playing a primary role in the development of DG-deficient cardiomyopathy and the development of focal myocardial fibrosis. The relatively slow progression of the cardiac disease in MLC2vcre-L/L mice may be attributable to many cells in the patches with membrane damage undergoing successful plasma membrane repair resulting in fewer cells with permanent damage.

In the working myocardium, cardiac myocytes are attached to neighboring cells by interacting laterally with matrix that separates adjacent cells and longitudinally through intercalated disks that mechanically and electrically connect neighboring cells. If isolated membrane damage in a single cell results in transient or permanent contractile failure, the surrounding myocytes may experience increased mechanical load. In the absence of stabilizing lateral interactions of those myocytes with extracellular matrix, this may result in inappropriate stretch or strain on neighboring myocytes that leads to damage of the sarcolemma. The localization of DG to costameres in striated muscle places DG at an important location for stabilizing myocytes, the sarcolemma, and their sarcomeres against mechanical activity or stretch. Dystrophin-deficient skeletal muscle has been shown to be particularly sensitive to the damaging effects of lengthening contrac-

tions.[23] Other matrix receptors in muscle, such as integrins, may also provide a parallel pathway toward in stabilizing cardiac myocytes. The combined loss of dystrophin and integrin in myocytes results in a more severe histological phenotype than the loss of either gene alone, especially under conditions of stress such as isoproterenol infusion.[24] It is possible that other mechanisms may be involved, including increased sensitivity of DG-deficient myocytes to circulating factors released by myocytes with membrane damage. We noted the patches of membrane damage also appeared to be limited to myocytes that were organized in similar orientations of their longitudinal axis (Figure 6), suggesting that the damage was related to orientation of the mechanical strain or stretch and not simply diffusion of molecules to neighboring cells.

A qualitative comparison of the histopathologic cardiac phenotypes of MLC2vcre-L/L mice (Figure 3), the phenotypes of *myd* mice (Figure 1 and Online Figure IV), and previous studies in dystrophin-deficient *mdx* mice suggests that MLC2vcre-L/L mice may have a more severe cardiac phenotype than both *myd* and *mdx* mice. This could be attributable to the fact that *myd* mice retain DG protein expression and preserve some of the intracellular functions of the DGC[21,22] Alternatively, the lack of skeletal muscle disease in MLC2vcre mice may result in increased locomotor activity and added stress on the heart as compared to other dystrophic mouse models. Dystrophic *mdx* mice fatigue very quickly,[22] and *myd* mice have observable reduced mobility and hindlimb paralysis caused by severe dystrophy and peripheral nerve dysfunction. Rescue of skeletal muscle disease in *mdx* mice by a skeletal muscle–specific minidystrophin transgene has been shown to lead to increased voluntary activity and a worse cardiac phenotype, possibly caused by increased stress placed on these hearts.[25] Therefore, there may be a paradoxical inverse relationship between cardiac disease severity in dystrophic models and the good health of skeletal muscle. This would fit well with our observation that acute exercise appears to increase the number of patches of cell membrane damage in MLC2vcre mice. Although *myd* mice are a genetic model of the relatively rare congenital muscular dystrophy MDC1D, the loss of DG glycosylation and the function of DG as an extracellular matrix receptor is so far biochemically identical to many forms of glycosylation-deficient muscular dystrophy including the relatively common LGMD2I.[10] Our results suggest that if a specific genetic disruption of this glycosylation pathway affected DG matrix receptor function in cardiac myocytes, this would likely lead to increased susceptibility to activity-induced myocardial damage and cardiovascular disease in human patients.

Acknowledgments

We thank Sally Prouty for technical assistance and the University of Iowa Hybridoma Facility for preparing the antibody IIH6. We thank the Nathan Shock Center In Vivo Functionality Core and Center for Integrative Genomics at the University of Michigan for support. We thank members of the Michele laboratory and Campbell laboratory for critical comments on the manuscript.

Sources of Funding

This work is funded by a Grant-in-Aid from the American Heart Association and NIH grant R01-HL080388 (to D.E.M.); an American Heart Association Postdoctoral Fellowship (to Z.K.); and NIH grant RR017369 (to R.M.W.). This work was supported in part by the Senator Paul D. Wellstone Muscular Dystrophy Cooperative Research Center grant 1 U54 NS053672. K.P.C. is an investigator of the Howard Hughes Medical Institute.

Disclosures

None.

References

1. Finsterer J, Stollberger C. The heart in human dystrophinopathies. *Cardiology*. 2003;99:1–19.
2. Coral-Vazquez R, Cohn RD, Moore SA, Hill JA, Weiss RM, Davisson RL, Straub V, Barresi R, Bansal D, Hrstka RF, Williamson R, Campbell KP. Disruption of the sarcoglycan-sarcospan complex in vascular smooth muscle: a novel mechanism for cardiomyopathy and muscular dystrophy. *Cell*. 1999;98:465–474.
3. Durbeej M, Cohn RD, Hrstka RF, Moore SA, Allamand V, Davidson BL, Williamson RA, Campbell KP. Disruption of the beta-sarcoglycan gene reveals pathogenetic complexity of limb-girdle muscular dystrophy type 2E. *Mol Cell*. 2000;5:141–151.
4. Nigro V, Okazaki Y, Belsito A, Piluso G, Matsuda Y, Politano L, Nigro G, Ventura C, Abbondanza C, Molinari AM, Acampora D, Nishimura M, Hayashizaki Y, Puca GA. Identification of the Syrian hamster cardiomyopathy gene. *Hum Mol Genet*. 1997;6:601–607.
5. Thomas GD, Sander M, Lau KS, Huang PL, Stull JT, Victor RG. Impaired metabolic modulation of alpha-adrenergic vasoconstriction in dystrophin-deficient skeletal muscle. *Proc Natl Acad Sci U S A*. 1998;95:15090–15095.
6. Heydemann A, Huber JM, Kakkar R, Wheeler MT, McNally EM. Functional nitric oxide synthase mislocalization in cardiomyopathy. *J Mol Cell Cardiol*. 2004;36:213–223.
7. Wheeler MT, Allikian MJ, Heydemann A, Hadhazy M, Zarnegar S, McNally EM. Smooth muscle cell-extrinsic vascular spasm arises from cardiomyocyte degeneration in sarcoglycan-deficient cardiomyopathy. *J Clin Invest*. 2004;113:668–675.
8. Tsubata S, Bowles KR, Vatta M, Zintz C, Titus J, Muhonen L, Bowles NE, Towbin JA. Mutations in the human delta-sarcoglycan gene in familial and sporadic dilated cardiomyopathy. *J Clin Invest*. 2000;106:655–662.
9. Straub V, Ettinger AJ, Durbeej M, Venzke DP, Cutshall S, Sanes JR, Campbell KP. epsilon-sarcoglycan replaces alpha-sarcoglycan in smooth muscle to form a unique dystrophin-glycoprotein complex. *J Biol Chem*. 1999;274:27989–27996.
10. Michele DE, Barresi R, Kanagawa M, Saito F, Cohn RD, Satz JS, Dollar J, Nishino I, Kelley RI, Somer H, Straub V, Mathews KD, Moore SA, Campbell KP. Post-translational disruption of dystroglycan-ligand interactions in congenital muscular dystrophies. *Nature*. 2002;418:417–422.
11. Grewal PK, Holzfeind PJ, Bittner RE, Hewitt JE. Mutant glycosyltransferase and altered glycosylation of alpha-dystroglycan in the myodystrophy mouse. *Nat Genet*. 2001;28:151–154.
12. Barresi R, Michele DE, Kanagawa M, Harper HA, Dovico SA, Satz JS, Moore SA, Dumanski JP, Schachter H, Cohn RD, Nishino I, Campbell KP. LARGE functionally bypasses alpha-dystroglycan glycosylation defects in congenital muscular dystrophies. *Nat Med*. 2004;10:696–703.
13. Holzfeind PJ, Grewal PK, Reitsamer HA, Kechvar J, Lassmann H, Hoeger H, Hewitt JE, Bittner RE. Skeletal, cardiac and tongue muscle pathology, defective retinal transmission, and neuronal migration defects in the Large(myd) mouse defines a natural model for glycosylation-deficient muscle-eye-brain disorders. *Hum Mol Genet*. 2002;11:2673–2687.
14. Hayashi YK, Ogawa M, Tagawa K, Noguchi S, Ishihara T, Nonaka I, Arahata K. Selective deficiency of alpha-dystroglycan in Fukuyama-type congenital muscular dystrophy. *Neurology*. 2001;57:115–121.
15. Chen J, Kubalak SW, Chien KR. Ventricular muscle-restricted targeting of the RXRalpha gene reveals a non-cell-autonomous requirement in cardiac chamber morphogenesis. *Development*. 1998;125:1943–1949.

16. Regan CP, Manabe I, Owens GK. Development of a smooth muscle-targeted cre recombinase mouse reveals novel insights regarding smooth muscle myosin heavy chain promoter regulation. *Circ Res*. 2000;87:363–369.
17. Moore SA, Saito F, Chen J, Michele DE, Henry MD, Messing A, Cohn RD, Ross-Barta SE, Westra S, Williamson RA, Hoshi T, Campbell KP. Deletion of brain dystroglycan recapitulates aspects of congenital muscular dystrophy. *Nature*. 2002;418:422–425.
18. Weiss RM, Ohashi M, Miller JD, Young SG, Heistad DD. Calcific aortic valve stenosis in old hypercholesterolemic mice. *Circulation*. 2006;114:2065–2069.
19. Pandya K, Kim HS, Smithies O. Fibrosis, not cell size, delineates beta-myosin heavy chain reexpression during cardiac hypertrophy and normal aging in vivo. *Proc Natl Acad Sci U S A*. 2006;103:16864–16869.
20. Towbin JA, Bowles NE. Molecular genetics of left ventricular dysfunction. *Curr Mol Med*. 2001;1:81–90.
21. Higginson JR, Winder SJ. Dystroglycan: a multifunctional adaptor protein. *Biochem Soc Trans*. 2005;33(pt 6):1254–1255.
22. Kobayashi YM, Rader EP, Crawford RW, Iyengar NK, Thedens DR, Faulkner JA, Parikh SV, Weiss RM, Chamberlain JS, Moore SA, Campbell KP. Sarcolemma-localized nNOS is required to maintain activity after mild exercise. *Nature*. 2008;456:511–515.
23. Dellorusso C, Crawford RW, Chamberlain JS, Brooks SV. Tibialis anterior muscles in mdx mice are highly susceptible to contraction-induced injury. *J Muscle Res Cell Motil*. 2001;22:467–475.
24. Elsherif L, Huang MS, Shai SY, Yang Y, Li RY, Chun J, Mekany MA, Chu AL, Kaufman SJ, Ross RS. Combined deficiency of dystrophin and beta1 integrin in the cardiac myocyte causes myocardial dysfunction, fibrosis and calcification. *Circ Res*. 2008;102:1109–1117.
25. Townsend D, Yasuda S, Li S, Chamberlain JS, Metzger JM. Emergent dilated cardiomyopathy caused by targeted repair of dystrophic skeletal muscle. *Mol Ther*. 2008;16:832–835.

SUPPLEMENT MATERIAL

DETAILED METHODS

Mice. Homozygous *myd* mice were generated from mating heterozygous mice in a colony of B6C3Fe-a/a-LARGE*myd* mice originally purchased from Jackson Laboratories. Mice homozygous for the floxed allele of the DAG1 gene were previously described(1). Transgenic mice that express cre recombinase in ventricular cardiac myocytes under control of the myosin light chain 2v regulatory region (MLC2vcre) were a kind gift from Dr. Kenneth Chien (Harvard University) (2). Mice expressing cre recombinase in smooth muscle cells under the control of the smooth muscle myosin heavy chain promoter were a kind gift from Dr. Gary Owens (University of Virginia) (3). Mice deficient for DAG1 were generated by mating male mice that were heterozygous for the cre transgene and homozyogous for the DAG1 floxed allele with females that were homozyogous for the DAG1 floxed allele, and mice were born from these crosses with normal Mendelian ratios. Analysis of several litters from crosses of MLC2vcre mice where 50% of the offspring were predicted to carry the transgene showed 42/76 mice carried the MLC2vcre transgene. Analysis of several litters from crosses of SMMHC mice where 50% of the offspring were predicted to carry the transgene showed 17/36 mice carried the SMMHCcre transgene. All comparisons were made on age and sex matched littermate mice.

Dystroglycan glycosylation, protein expression and laminin binding activity. Dystroglycan glycosylation and protein expression were analyzed using a combination of a glycosylation- sensitive dystroglycan antibody (IIH6) and dystroglycan antibodies (SHP5ADG) which recognize the core protein of α-DG, and AP83 or NCL-b-DG(Novocastra) which recognizes α-DG) as previously described (4). Briefly, tissues were homogenized in Tris buffered saline, pH 7.5 (TBS) containing 1% TX-100 using 1mL per 100mg tissue. Solubilized glycoproteins were enriched with wheat germ agglutin (WGA, Vector Laboratories) agarose beads and eluted with TBS containing 0.1% TX-100 and 0.5 M N-acetlyglucosamine. Samples were analyzed using 3-15% SDS-PAGE followed by Western blotting. Dystroglycan specific laminin binding activity was measured with blot overlay assays using purified laminin-1 as described (4). Total laminin binding activity in the glycoprotein preparations was measured using solid phase binding analysis as previously described(4). Briefly, WGA glycoproteins were diluted 1:50 in TBS and coated on Costar RIA-ELISA plates. Following washing and treatment with blocking buffer (TBS + 3% BSA + 0.1% Tween 20), plates were incubated with purified laminin-1 diluted in blocking buffer containining either 1mM $CaCl_2$ or 5mM EDTA. Bound laminin was detected by sequential application of a rabbit polyclonal anti-laminin antibody (Sigma) in blocking buffer and an anti-rabbit IgG conjugated to horseradish peroxidase (Jackson Immunochemicals). Plates were developed with 0-phenylenediamine/dihyrogen peroxide in citrate buffer, pH 5.0 and reactions were terminated with sulfuric acid. Colorimetric quantification was performed on a Biorad Benchmark Plus microplate reader.

For quantifying the expression dystrophin glycoprotein complex and dysferlin in gene targeted mice, ventricles were homogenized in 1% TX-100, total protein was quantified using DC Protein Assay (Biorad) for normalization, and samples were analyzed by 3-15% SDS PAGE and Western blots as described above. Monococlonal antibodies against β-SG and dysferlin monoclonal antibodies were obtained from Novacastra.

Morphological characterization and immunohistochemistry

Hearts were removed from anesthetized mice, atria and greater vessels were removed, blood was removed from the chamber by wicking, and the wet heart weight was obtained. For histology, mice were perfused with formalin followed by removal of the heart, paraffin embedding and sectioning. For routine histology, 4 micron sections were stained with hematoxylin and eosin. For characterization of fibrosis, sections were stained with 0.1% picrosirius red/0.1% Fast Green. For quantification of fibrotic areas, ventricular chamber cross sections sections were analyzed by ImageJ to quantify picrosirius red stained areas and normalized to the total cross sectional area of the heart. For immunofluorescence localization,

hearts were removed and frozen in liquid nitrogen-cooled isopentane. Eight micron fresh cyrosections were fixed in 3% paraformaldehyde, blocked with PBS + 3% BSA and were stained with dystroglycan antibodies diluted in blocking buffer followed by incubation with Cy3-conjugated secondary antibodies (Jackson Immunochemicals).

In vivo echocardiography. Mice were analyzed by *in vivo* echocardiography while conscious as described (5). Mice were lightly sedated with midazolam (0.15 mg SC). A 15-MHz linear-array probe was applied horizontally to the chest with the mouse held by the nape of the neck and cradled in the imager's hand. The imaging probe was coupled to a Sonos 5500 imager (Philips Medical Systems, Bothell, Wash), which generated ≈180 to 200 2-dimensional frames per second. Images were acquired in both short- and long-axis left ventricular (LV) planes. Pulse-wave Doppler tracings were measured near the ventricular aspect of the mitral valve to measure heart rate. All images were acquired and then analyzed offline with the imager blinded to mouse genotype. Endocardial and epicardial borders were traced in the short-axis plane at end diastole and end systole using custom designed software (Freeland Medical Systems, Louisville, Colo). The lengths from the left ventricular outflow tract to the endocardial apex and the epicardial apex, respectively, were measured at end diastole and end systole. Left ventricular mass, end diastolic left ventricular volume, and end-systolic left ventricular volume were calculated by the biplane area-length method(6).

RT PCR for pathological markers of cardiomyopathy. Total RNA was isolated from snap frozen heart samples using TRIzol reagent (Invitrogen), DNase treated and purified with Qiagen RNeasy Mini Kit. Only RNA samples with absorbance ratios 260/280 nm between 1.8 and 2.2 and reserved RNA integrity as checked by denaturing agarose gel electrophoresis were used for further experiments. cDNA was synthesized from 0.6 µg of total RNA using High Capacity cDNA Reverse Transcription kit (Applied Biosystems). Real-time PCR experiments were performed using SYBR Green chemistry on iCycler iQ Detection System (Biorad). Primer sets for mouse atrial natriuretic factor (NPPA) and beta-2-microglobulin (B2M) gene were designed using the Primer Express 1.5 software according to Applied Biosystems' guidelines. The primers were as follows: NPPA forward/reverse 5'-CCATATTGGAGCAAATCCTGTGT-3'/5'-CTTCTACCGGCATCTTCTCCTC-3'; B2M forward/reverse 5'-TCTTTCTGGTGCTTGTCTCACTG-3'/5'- GTTCGGCTTCCCATTCTCC-3'. For the β-myosin heavy chain gene,primers published by Gaussin et al (7) were used . B2M was selected as an endogenous reference based on literature survey (8-10). A threshold cycle (C_t) value of *B2M* and a target gene was measured at least in two independent runs, each time in triplicate. To quantify a relative change in gene expression, the comparative C_t method was used (11). All comparisons were done using unpaired two-tail unequal variance *t*-test with a significance threshold of $P<0.05$.

In vivo assessment of myocardial membrane damage. Mice with cardiac specific dystroglycan gene disruption and wild-type littermates, <5 months of age, were subjected to a single bout of 1-hour long running on a treadmill with an in-built shock grid with 5 degree inclination. Initial running speed of 7 m/min was increased every 2 minutes by 3 m/min until the maximal speed without signs of exhaustion or refusal to run (~16m/min) was achieved. Five hours before the exercise session, mice were given an i.p. injection of 0.1 mg/ g Evans blue dye in saline. Next morning after exercise completion (~18 h), hearts were removed from anesthetized animals and frozen in isopentane cooled in liquid nitrogen. A set of non-exercised mutant and wild-type mice were injected with Evans blue dye and their hearts were collected the same way as for exercised animals. Frozen heart samples were sectioned at 8 microns in a cryostat. From each heart, 4 cross-sections >250-300 microns apart were obtained. Immunostaining with anti-laminin 1 antibody (Sigma, 1:1000) and secondary antibody conjugated to Alexa 488 (Molecular probes, 1:800) was used to show cell boundaries on Evans blue treated tissue. Each slide was scored for Evans blue positive cells using an Olympus BX51 microscope (Olympus, Tokyo, Japan).

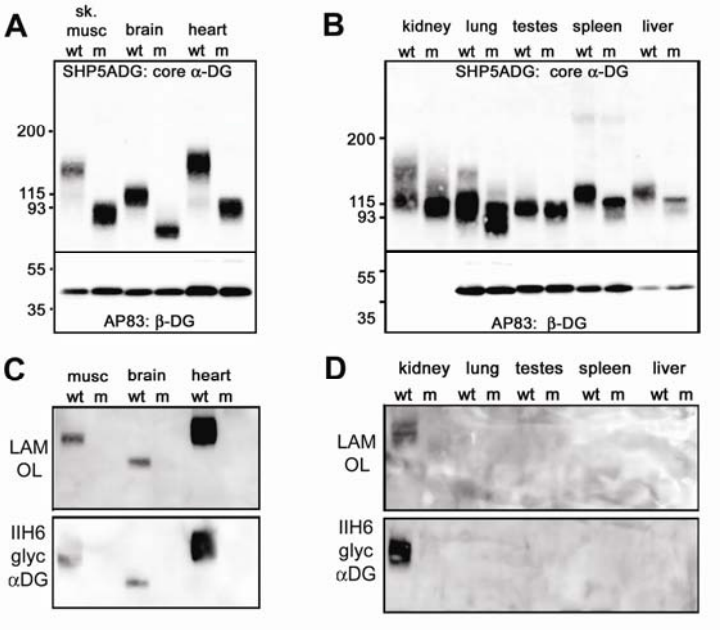

Online Figure 1. Distribution of dystroglycan glycosylation in tissues of WT and LARGE *myd* mice. In this series of experiments, WGA enriched extracts were prepared from individual tissues from WT (w) and *myd* (m) mice and the Western blots and overlay assays were performed on replicate blots shown in panels A-D. Therefore, the reactivity of the IIH6 antibody recognizing the glycosylated alpha dystroglycan (glyc. α-DG) and laminin overlay assays (LAM OL) can be compared to amount of alpha dystroglycan recognized by the core alpha dystroglycan peptide antibody (SHP5ADG) in the data series shown. Sk. Musc, hindlimb skeletal muscle, AP83 β-DG, beta-dystroglycan peptide antibody; **A and B)** Assessment of □DG protein expression in tissues of *myd* mice by Western blotting using an antibody that recognizes the core □DG protein shows dramatic changes in molecular weight are largely confined to muscle and brain tissues. **C and D)** The fully glycosylated α-DG (recognized by IIH6) and laminin binding glycoform (determined by laminin overlay assay) of α-DG are easily detected in muscle tissues, brain and kidney but not in other tissues of wild-type mice, nor in any tissues from *myd* mice. The reason for the failure to detect of beta-DG in kidney is unclear but may represent differential proteolytic cleavage of beta DG in kidney.

Supplemental Information for Online Figure 1. The characterization of the requirement for LARGE for the functional modification of dystroglycan across tissues (Figure 1, Suppemental Figure 1), suggests that loss of LARGE has the greatest impact on glycosylation in skeletal muscle, cardiac muscle, smooth muscle, and nervous system, and that it also has some impact in the kidney while other tissues are generally less affected. Notably, most of the tissues in which the apparent molecular weight of □-DG are not significantly affected by the LARGE mutation, the molecular weight α-DG is fairly low, and IIH6 reactivity and laminin binding activity are virtually not detectable. Whether these low molecular weight, non laminin binding glycoforms of α-DG have a functional role in non-muscle tissues is not clear. The molecular basis for the heterogeneity of dystroglycan glycosylation in different tissues is also not known. Even in the LARGE deficient *myd* mice, the heterogeneity of dystroglycan glycosylation in different tissues is quite pronounced (Figure 1, Supplemental Figure 1) indicating while LARGE dependent glycosylation is very important for laminin binding activity, it is not the only factor that contributes to the

tissue heterogeneity of dystroglycan glycosylation. In the mouse genome, there is a homologue for LARGE called LARGE2, that is able to glycosylate α-DG and induce laminin binding activity when overexpressed in cultured cells (12). However, our results suggest that the endogenous activity of LARGE2 in adult animals is probably insufficient because all tissues tested that showed significant amounts of highly glycosylatd dystroglycan in WT mice, show dramatic loss of dystroglycan glycosylation and function in LARGE deficient *myd* mice. *Myd* mice, which carry a large null deletion in the LARGE gene can survive to live birth and beyond. This is in stark contrast to the dystroglycan, fukutin and POMT1 knockout mice which are all embryonic lethal at E9.5(13-15). Therefore, it remains possible that LARGE2 is required, or may compensate for loss of LARGE, with respect to the dystroglycan glycosylation events that are critical during mouse development.

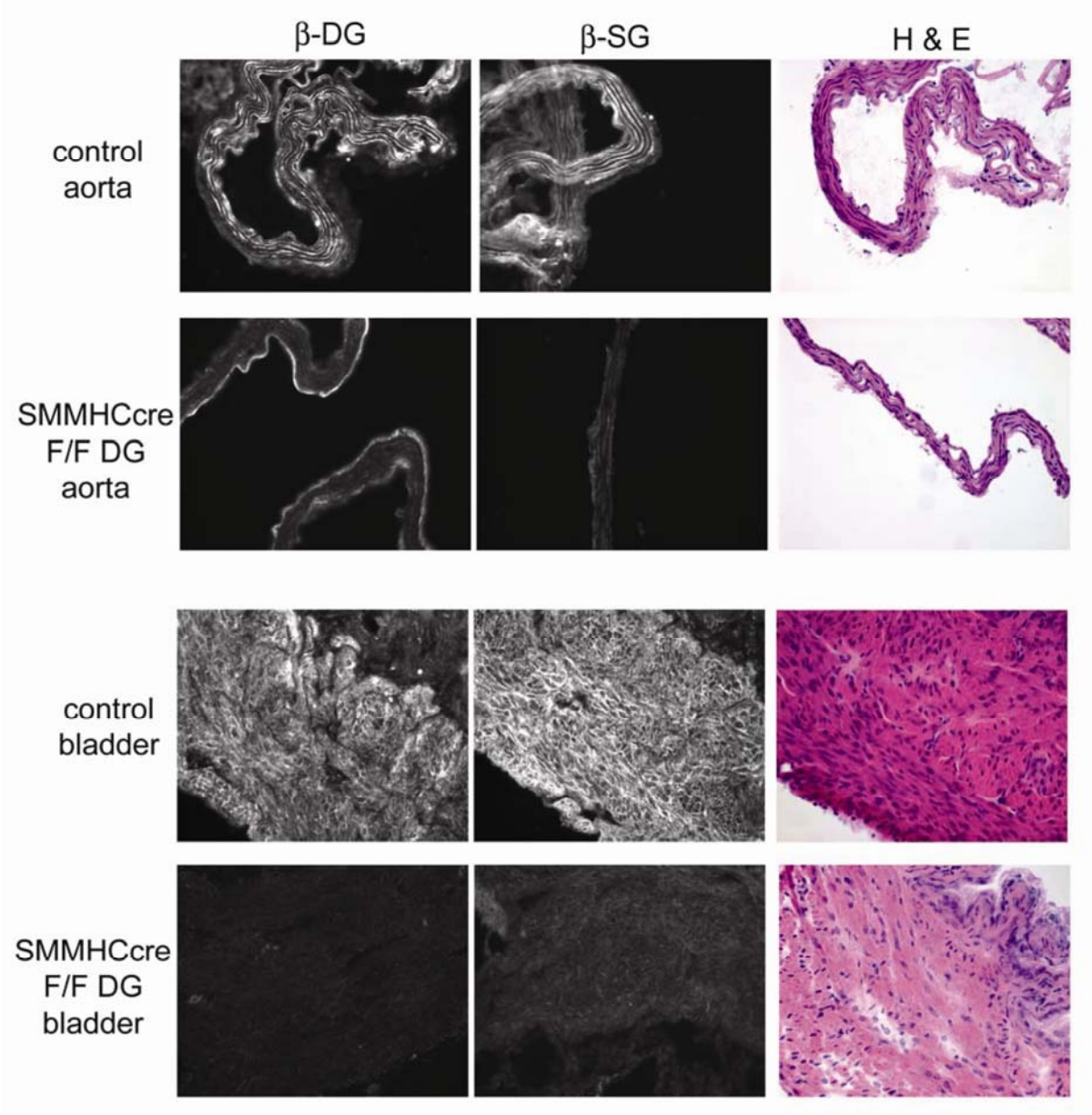

Online Figure 2. Targeted deletion of dystroglycan in smooth muscle leads to a marked reduction in sarcoglycan expression in smooth muscle. Immunostaining of β-DG and β -sarcoglycan in frozen sections of aorta and smooth muscle of SMMHCcre-L/L mice.

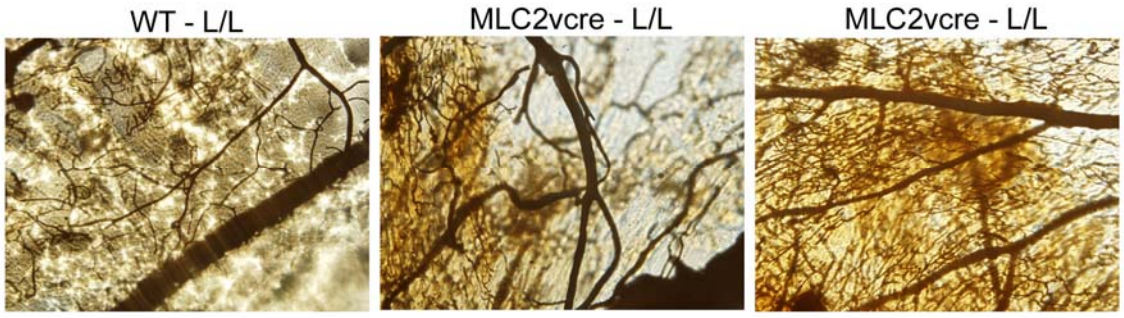

Online Figure 3. Microfil perfusion experiments at 8 months of age do not show evidence of coronary vasopasm in MLC2vcre-L/L mice compared to WT-L/L littermates.
Mice were perfused with Microfil MV-122 by cardiac puncture, and hearts were cleared with graded solutions of ethanol and methyl salicyclate as described by the manufacturer (Flowtech, Inc.) Thick sections were obtained and viewed on a Olympus BX-51 upright microscope.

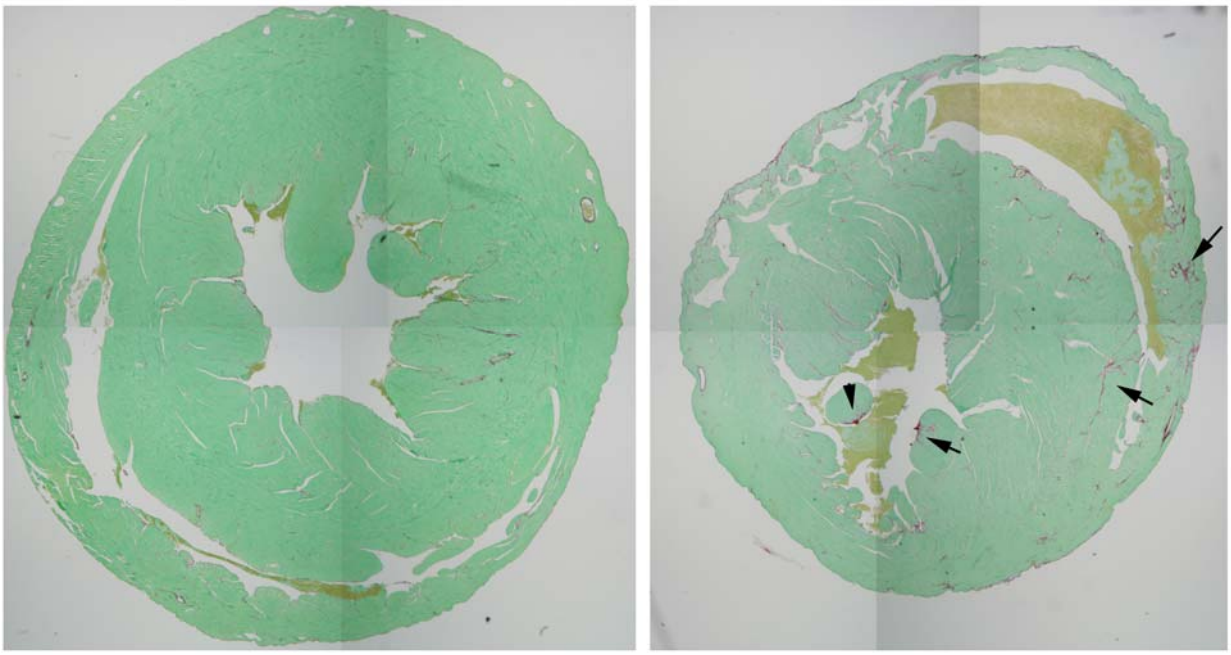

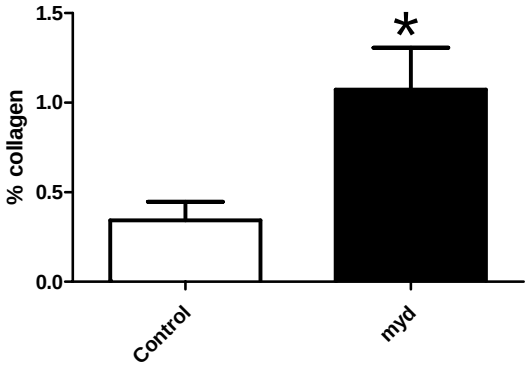

Supplemental Figure 4. Representative entire cross sections of myocardium from *myd* mice and littermate control mice at 50 weeks of age. Focal deposition of interstitial collagen is observed in both left and right ventricles (arrows) of myd mice, but overall the phenotype appears milder than that observed in 50 week old MLC2vcre-L/L mice (shown in figure 3). Image analysis indicted the total area of collagen deposition was significantly increased in *myd* mice compared to littermate control mice (data are mean +/- SEM, *=p<0.05, n=3). While some perivascular collagen is observed in both WT and myd animals, the increase observed in collagen in myd animals is primarily due to increase in interstitial collagen.

REFERENCES FOR SUPPLEMENT

1. Moore, S.A., Saito, F., Chen, J., Michele, D.E., Henry, M.D., Messing, A., Cohn, R.D., Ross-Barta, S.E., Westra, S., Williamson, R.A., et al. 2002. Deletion of brain dystroglycan recapitulates aspects of congenital muscular dystrophy. *Nature* 418:422-425.
2. Chen, J., Kubalak, S.W., and Chien, K.R. 1998. Ventricular muscle-restricted targeting of the RXRalpha gene reveals a non-cell-autonomous requirement in cardiac chamber morphogenesis. *Development* 125:1943-1949.
3. Regan, C.P., Manabe, I., and Owens, G.K. 2000. Development of a smooth muscle-targeted cre recombinase mouse reveals novel insights regarding smooth muscle myosin heavy chain promoter regulation. *Circ Res* 87:363-369.
4. Michele, D.E., Barresi, R., Kanagawa, M., Saito, F., Cohn, R.D., Satz, J.S., Dollar, J., Nishino, I., Kelley, R.I., Somer, H., et al. 2002. Post-translational disruption of dystroglycan-ligand interactions in congenital muscular dystrophies. *Nature* 418:417-422.
5. Weiss, R.M., Ohashi, M., Miller, J.D., Young, S.G., and Heistad, D.D. 2006. Calcific aortic valve stenosis in old hypercholesterolemic mice. *Circulation* 114:2065-2069.
6. Hill, J.A., Karimi, M., Kutschke, W., Davisson, R.L., Zimmerman, K., Wang, Z., Kerber, R.E., and Weiss, R.M. 2000. Cardiac hypertrophy is not a required compensatory response to short-term pressure overload. *Circulation* 101:2863-2869.
7. Gaussin, V., Tomlinson, J.E., Depre, C., Engelhardt, S., Antos, C.L., Takagi, G., Hein, L., Topper, J.N., Liggett, S.B., Olson, E.N., et al. 2003. Common genomic response in different mouse models of beta-adrenergic-induced cardiomyopathy. *Circulation* 108:2926-2933.
8. Mahoney, D.J., Carey, K., Fu, M.H., Snow, R., Cameron-Smith, D., Parise, G., and Tarnopolsky, M.A. 2004. Real-time RT-PCR analysis of housekeeping genes in human skeletal muscle following acute exercise. *Physiol Genomics* 18:226-231.
9. Lupberger, J., Kreuzer, K.A., Baskaynak, G., Peters, U.R., le Coutre, P., and Schmidt, C.A. 2002. Quantitative analysis of beta-actin, beta-2-microglobulin and porphobilinogen deaminase mRNA and their comparison as control transcripts for RT-PCR. *Mol Cell Probes* 16:25-30.
10. Kuhn, M., Voss, M., Mitko, D., Stypmann, J., Schmid, C., Kawaguchi, N., Grabellus, F., and Baba, H.A. 2004. Left ventricular assist device support reverses altered cardiac expression and function of natriuretic peptides and receptors in end-stage heart failure. *Cardiovasc Res* 64:308-314.
11. Livak, K.J., and Schmittgen, T.D. 2001. Analysis of relative gene expression data using real-time quantitative PCR and the 2(-Delta Delta C(T)) Method. *Methods* 25:402-408.
12. Grewal, P.K., McLaughlan, J.M., Moore, C.J., Browning, C.A., and Hewitt, J.E. 2005. Characterization of the LARGE family of putative glycosyltransferases associated with dystroglycanopathies. Glycobiology 15:912-923.
13. Kurahashi, H., Taniguchi, M., Meno, C., Taniguchi, Y., Takeda, S., Horie, M., Otani, H., and Toda, T. 2005. Basement membrane fragility underlies embryonic lethality in fukutin-null mice. Neurobiol Dis 19:208-217.
14. Willer, T., Prados, B., Falcon-Perez, J.M., Renner-Muller, I., Przemeck, G.K., Lommel, M., Coloma, A., Valero, M.C., de Angelis, M.H., Tanner, W., et al. 2004. Targeted disruption of the Walker-Warburg syndrome gene Pomt1 in mouse results in embryonic lethality. Proc Natl Acad Sci U S A 101:14126-14131.
15. Williamson, R.A., Henry, M.D., Daniels, K.J., Hrstka, R.F., Lee, J.C., Sunada, Y., Ibraghimov-Beskrovnaya, O., and Campbell, K.P. 1997. Dystroglycan is essential for early embryonic development: disruption of Reichert's membrane in Dag1-null mice. Human Molecular Genetics 6:831-841.